Available online at www.sciencedirect.com
SCIENCE DIRECT®
Journal of Power Sources 146 (2005) 71–78
JOURNAL OF POWER SOURCES
www.elsevier.com/locate/jpowsour

A review on new solutions, new measurements procedures and new materials for rechargeable Li batteries

D. Aurbach *

Department of Chemistry, Bar-Ilan University, Ramat-Gan 52900, Israel

Available online 31 May 2005

Abstract

We describe herein approaches for R&D of improved solutions for Li-ion batteries, new concepts for measuring aging processes of Li-ion battery electrodes and approaches for the synthesis of novel electrode materials for Li-ion batteries. We demonstrate the possibility of successfully using standard $LiPF_6$ solutions for Li-ion batteries at elevated temperatures by the use of organosilicon additives. We also show how these solutions are compatible for 5 V systems. We show how measurements of the self-discharge current of lithiated graphite electrodes during cycling, reflect the complicated aging of the electrodes, and we map the various processes that influence the overall aging trends observed. Several novel approaches for the synthesis of nanomaterials for Li-ion batteries, including carbonaceous materials, tin-based compounds and transition metal oxides, are described. These include soft reactions in the liquid phase, high temperature reactions under autogenic pressure and the use of microwave radiation and sonochemistry.

Keywords: Li-ion batteries; $LiPF_6$ electrolyte solutions; 5 V systems; Self-discharge; Aging; Nanomaterials

1. Introduction

The commercialization of rechargeable Li-ion batteries in recent years, and the success of this technology in conquering the battery market, is driving the scientific and technological communities towards even more efforts to develop new solutions and materials for new and future generations of Li-ion batteries. The challenges are, naturally, to achieve higher energy density, higher rates, higher stability, longer cycle and calendar life, and improved safety. These demands create strong incentives for the promotion of first rate basic studies in materials science, surface science, crystallography, spectroscopy, microscopy and, of course, electrochemistry. We should mention the development of novel, high capacity negative electrodes based on amorphous silicon [1], tin alloys [2], nanoparticles of transition metal oxides (low oxidation state of the transition metal) [3], inter-metallic compounds [4] and new carbonaceous materials [5]. Intensive and prolific efforts are in progress to develop new electrolyte solutions with non-flammable solvents [6], safer salts such as Li-bi oxalato-borate (LiBOB) [7] and over charge protection [8]. Efforts are underway to develop new separators [9] and new solid state electrolytes, both polymeric [10] and ceramic [11]. Finally, there are highly intensive efforts to develop new cathode materials such as olivines [12], layered $LiM_{1_x}M_{2_y}M_{3_z}O_2$ of high redox potentials [13] and $LiMn_{2-x}M_xO_4$ spinel compounds of high redox potentials [14].

Intensive efforts are underway to understand all the fine details regarding the structure of these materials, their surface chemistry and the correlation between these details and the electrochemical behavior of electrode materials. The use of novel methods such as solid state NMR [15], neutron diffraction [16], XANES [17], EXAFS [18] and in situ techniques (e.g., Raman [19], FTIR [20], SPM [21], XRD [22] and MS [23]) contributes a great deal to high level research in that field. Another important breakthrough in the field that should be acknowledged is the intensive and highly successful use of computational chemistry for the prediction of bulk structures [24] and interfacial interactions [25].

* Tel.: +972 3 531 8317; fax: +972 3 535 1250.
E-mail address: aurbach@mail.biu.ac.il.

0378-7753/$ – see front matter © 2005 Elsevier B.V. All rights reserved.
doi:10.1016/j.jpowsour.2005.03.151

All the references cited above are only limited examples of the basic and intensive studies that are dedicated to the advance of Li battery technology.

In this paper, we would like to describe in brief some recent contributions of the electrochemistry group at Bar-Ilan University to the science of Li batteries, R&D of new solutions, new measurement procedures and new synthesis routes of electrode materials.

2. Experimental

Electrolyte solutions comprising various alkyl carbonate solvents (EC, DMC, EMC, DEC, etc.) and $LiPF_6$ were obtained from Merck KGaA or from Tomiyama Inc. (Li battery grade), and could be used as received. Organosilicon additives were obtained from Aldrich Inc. and $LiMn_{1.5}Ni_{0.5}O_4$ electrodes were obtained from LG (Daejon, Korea). Various carbonaceous materials were obtained from companies such as Timrex Inc., Superior Graphite Inc. and Osaka Gas Inc. Precursors for different syntheses were obtained from Aldrich Inc. and Fluka Inc. Composite negative and positive electrodes comprising Cu and Al foil current collectors, respectively, coated with thin films containing the active mass (graphitic carbons or transition metal oxides), conductive additives (5–10%) in the case of positive electrodes and a PVdF binder (5–10%), were prepared as already described [26]. Most of the electrochemical measurements were carried out using a three-electrode cell configuration in coin-type cells from NRC Canada (Li foils, reference and counter electrodes). The electrochemical measurements were carried out using multichannel, computerized equipment from Maccor, Arbin, Solartron, EG&G and ECO Chemie, with the relevant software. All the preparations for the electrochemical and spectroscopic measurements were carried out in VAC Inc. glove boxes (highly pure argon atmosphere). Microscopic measurements were carried out using TEM, SEM and HRTEM equipment from JEOL Inc. The transfer method has already been described [27]. XPS measurements were carried out using the H-Axis system from Kratos Inc. Micro Raman measurements were carried out using equipment from Jobin-Ivon Inc. The element analysis of the solutions was carried out by atomic absorption (AA) and ICP (equipment from Perkin-Elmer Inc.).

3. Results and discussion

3.1. High performance of $LiPF_6$ solutions

The standard solutions used in Li-ion batteries, which usually comprise mixtures of alkyl carbonate solvents with EC as a necessary component, and $LiPF_6$ as an electrolyte, were developed based on systematic experiments and extensive work over more than two decades (1970–1990). Most of the negative electrodes for Li batteries (Li, Li alloys, lithiated carbonaceous materials, etc.) develop highly stable passivation in the standard solutions, based on reasonably stable surface films that are good Li-ion conductors [28]. On a thermodynamic basis, all negative electrodes for Li-ion batteries are highly reactive with all alkyl carbonates and with PF_6^- and its decomposition product, PF_5. Nevertheless, the metastability reached in all Li-ion battery systems in the negative electrode–solution interface, due to the formation of passivating surface films, is sufficient to allow the satisfactory performance of 4 V Li-ion batteries at ambient conditions (hundreds of cycles at 100% DOD, long calendar life, 1*C* rates and higher). In addition, it is clear that the standard solutions are compatible with all possible 4 V cathodes used or suggested for use in Li-ion batteries ($LiCoO_2$ in use, $LiMn_2O_4$ and its derivatives, $LiNiO_2$ and its derivatives, etc.). While there are obvious surface reactions between the above cathodic materials and standard solutions, including nucleophilic reactions [29], acid–base reactions [29] and transition metal dissolution [30], these surface reactions are usually minor and are not detrimental to the successful operation of Li-ion batteries. Hence, there are no measurable, pronounced reactions between 4 V cathodes and standard solutions at ambient temperatures. We should mention, however, that at elevated temperatures, there are pronounced redox reactions between the PF_6^- anion and the solvents [31] and between all the solution components and the cathode materials [32] with onsets >150 °C. The remaining major problems of the standard solutions are high temperature performance, compatibility with high voltage cathodes (e.g., 5 V substituted $Li_xMn_{2-y}M_yO_4$ spinel materials, M = Ni, Cu and Cr) and flammability. The above-mentioned metastability on which the successful operation of Li-ion batteries depends, results in a very delicate balance among many possible surface reactions on both anodes and cathodes. Therefore, replacement of the major components of standard solutions, e.g., solvents and salt, in order to improve the performance of the batteries beyond the present achieved performance, appears to be impractical. Hence, the practical challenge is to push to the utmost, the performance of current standard solutions, thus obtaining good performance at elevated temperatures and with high voltage cathode materials.

We discovered that the use of organosilicon compounds as additives (around 1%, v/v) can improve considerably the performance of Li-ion battery systems at elevated temperatures. Fig. 1 summarizes the results of several experiments with full Li-ion cells and with half cells at 60 °C. The systems studied included MCMB-graphite/EC-DMC-$LiPF_6$ 1 M/$LiCoO_2$, Li/standard solution/MCMB graphite and Li/standard solution/$LiCoO_2$ (coin-type cells). A moderate, but continuous, capacity-fading is observed when Li-ion cells are cycled at elevated temperatures. Testing half cells shows that the major capacity-fading observed is due to the anode side. Based on thermal studies of standard solutions [31], we suggest that small-scale redox reactions between PF_6^- or PF_5 and the solvent molecules produce HF, which reacts with major components in the passivating surface films

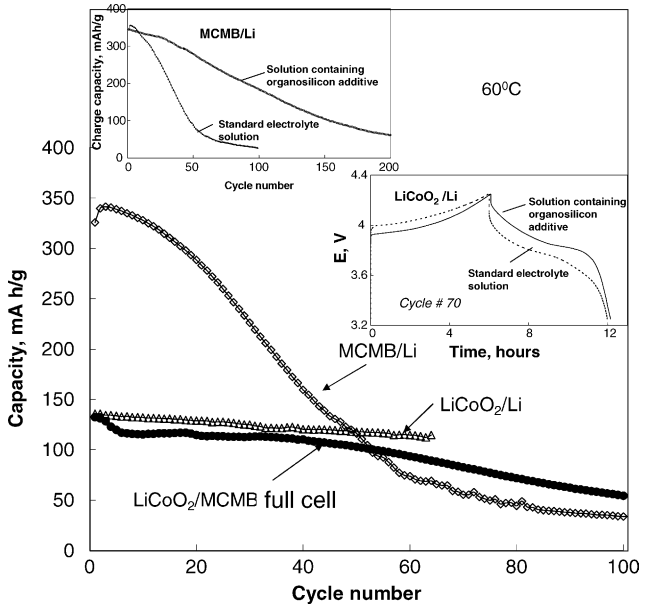

Fig. 1. A summary of experiments related to MCMB-$LiCoO_2$, MCMB-Li and $LiCoO_2$–Li cells with standard EC-DMC/$LiPF_6$ 1 M solutions and the same solution containing 1% of an R_4Si additive.

on the anode: ROLi, $ROCO_2Li$, Li_2O and LiOH, resulting in the precipitation of LiF [28]. Surface films comprising LiF as a major component are highly resistive to Li-ion migration [28]. These secondary reactions at elevated temperatures also lead to the electrical isolation of graphite particles. Thus, the performance of the anode side deteriorates upon cycling at elevated temperatures due to both the increase in impedance and the electrical disconnection of the active mass from the current collector. When the solutions contain organosilicon compounds, the latter react with trace HF and H_2O in the bulk and neutralize them from reacting on the electrodes' surface. Thereby, the performance of the anode size considerably improves at elevated temperatures with standard solutions containing R_4Si compounds. There is also a positive impact on the cathode side, as demonstrated in Fig. 1. However, here the impact is less pronounced, simply because the negative effect of species such as HF is less pronounced on the cathode side. In general, H^+ in solutions reacts with Li_xMO_2 oxides and lead to cation exchange, dissolution of M^{Z+} and, hence, detrimental changes in the structure of the active mass near the particles' surface. However, in the case of $LiCoO_2$ cathodes, the presence of Co^{2+} cations in solutions stabilizes the active mass and, thus, the negative effect of the presence of H^+ on the performance of $LiCoO_2$ cathodes is limited (because when Co ions dissolve and build up a steady concentration in the solution, the surface of the electrodes stabilizes [33]).

Fig. 2 demonstrates the ability to use $LiPF_6$-based solutions for 5 V Li-ion batteries. The figure summarizes many experiments with $LiNi_{0.5}Mn_{1.5}O_4$ spinel electrodes in EC-EMC/$LiPF_6$ solutions, in which the capacity of these electrodes (theoretical capacity of 158 mAh g^{-1}) was measured as a function of rate, cut-off voltage and temperature. An optimal performance was obtained when using 1.5 M $LiPF_6$ solutions. Since PF_6^- is the strongest oxidizer in these solutions, its high concentration increases the anodic stability of the solutions. The important message from these experiments, summarized in Fig. 2, is that a cut-off voltage of 4.85 V (versus Li/Li^+) is sufficient for extracting all the possible capacity from these electrodes at practical rates. At this potential, the solutions are stable and no detectable reactions between the electrodes and the solutions can be measured. $LiNi_{0.5}Mn_{1.5}O_4$ electrodes could

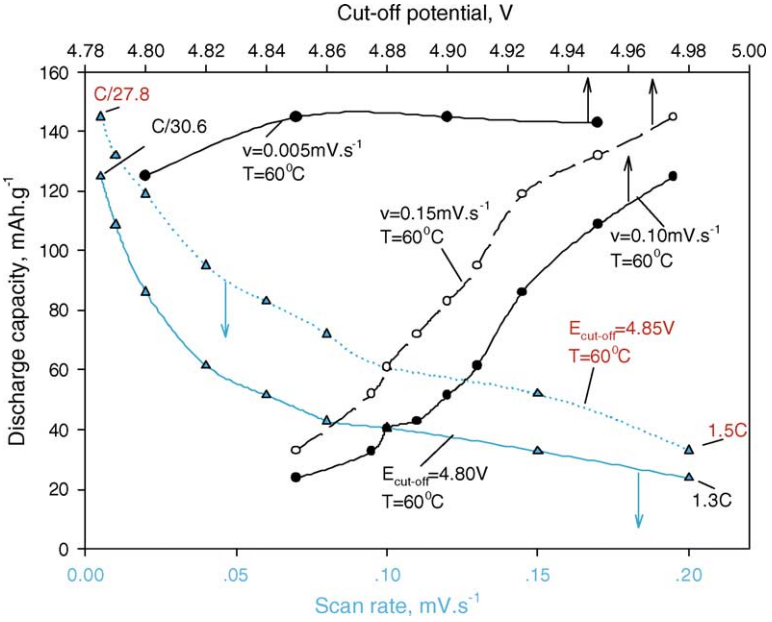

Fig. 2. A summary of experiments in which composite $LiNi_{05}Mn_{1.5}O_2$ electrodes were cycled (voltammetric measurements) in an EC-EMC/$LiPF_6$ 1.5 M solution. The capacity vs. cut-off potentials, scanning rates and temperature are indicated.

be cycled several hundred times in the above solution at 60 °C with relatively low capacity-fading (<0.3% loss per cycle) and very stable impedance characteristics.

The surface chemistry of these systems, which may lead to their stability, is currently being explored. The detrimental effects of the high concentration of $LiPF_6$ can be minimized by the use of additives, as discussed above (this is currently being studied).

3.2. A new measurement procedure: the study of self-discharge current as a diagnostic tool for aging processes

When graphite electrodes are fully lithiated (LiC_6), they are very strong reducing agents. The passivating, SEI type, surface films that cover the graphite particles (formed by the reduction of solution species at low potentials, in the presence of Li-ions [28]), never provide absolute passivation. Thereby, there are unavoidable, minor and small-scale self-discharge processes of lithiated graphite electrodes (corrosion cycles) in which electrons are injected into the solution phase through the surface films (tunneling processes), while Li-ions migrate in parallel through the surface films towards the film–solution interface, to complete the cycle. This process can be monitored by measuring the open circuit voltage of fully lithiated graphite electrodes, which always goes up upon storage at OCV conditions. The self-discharge current (I_{SD}) is a product of dE_{OCV}/dt and dQ/dE, where Q is the capacity of Li intercalation and its function of potential (E) is well known (e.g., from the integration of SSCV curves). We measured systematically the I_{SD} of various types of graphite electrodes (crystalline, synthetic flakes, natural graphite particles and MCMB) in their lithiated state, at various temperatures and during prolonged cycling. In a typical experiment, graphite electrodes were cycled galvanostatically or by voltammetry, hundreds of times, at 100% DOD in standard solutions (e.g., EC-DMC with $LiPF_6$). At the end of lithiation for each cycle, the self-discharge current as well as the impedance spectrum of the electrode were measured. After several selected cycles, slow scan rate cyclic voltammograms were measured, from which the kinetic behavior of the electrode upon cycling could be examined. Cycled electrodes were also measured by SEM and Raman spectroscopy. Hence, we accumulated a great deal of data for many electrode–solution systems that correlate capacity, self-discharge current, impedance behavior and kinetics, as a function of cycle number.

Fig. 3 provides a typical summary of such data (capacity and I_{SD} versus cycle number plus some selected impedance spectra and slow scan rate voltammograms). The capacity of all types of graphite electrodes usually fades very slightly in standard solutions, during prolonged cycling. The electrodes' impedance (surface film resistance and charge transfer resistance) decreases rapidly during initial cycling and then stabilizes (Fig. 3). The self-discharge current of these electrodes upon cycling always shows a peculiar (but consistent) behavior: it initially decreases and then after initial cycling, it stabilizes at low values. As cycling continues, I_{SD} increases after the first few dozen cycles and then stabilizes at relatively high values (see Fig. 3). This peculiar behavior can be explained in light of further spectroscopic and imaging results:

1. The surface films on graphite initially comprises Li organic salts, ROLi and $ROCO_2Li$ compounds. These surface species react with trace HF to form the corresponding acids, alcohols and LiF. Surface films on aged graphite electrodes in $LiPF_6$ solutions contain a high percentage of LiF and compounds of the Li_xPF_y and $Li_xPO_yF_z$ type.
2. During prolonged cycling, graphite crystallites become increasingly more cracked and disordered. We can even say that there is some amorphization of graphite near the surface crystallites. This is clearly evident by SEM (see Fig. 3) and by Raman spectroscopy, which clearly shows new bands that belong to disordered carbon, in the spectra of cycled electrodes.

Hence, the self-discharge currents of lithiated graphite electrodes that we measure during cycling is meaningful and reflects several aging processes that takes place in parallel, and that can be properly mapped, based on impedance, SSCV and spectroscopic studies.

There are two domains to be discussed: the aging processes of the surface films and the changes in the bulk graphite. The electrical properties of the surface films formed initially are obviously different from the surface films that develop during cycling. There are secondary reactions and dissolution–precipitation processes that bring the most insoluble species to the surface. If the active mass would be stable, the surface films should reach a steady state, with efficient passivating properties. Any tunneling of electron through the surface films results in the reduction of solution species that form insoluble products that block the holes. Hence, the I_{SD} should reach zero values upon aging if the surface films are laid on a stable substrate. However, the graphite particles are not stable. In addition to the periodic changes in volume upon a single lithiation–delithiation cycle, there are progressing changes during cycling: the capacity fades, not due to increasing kinetic limitations, as is evident from EIS and SSCV measurements, but rather due to changes in the active mass. Upon cycling, there is progressive cracking of the graphite particles and even some amorphization near the surface (Raman and SEM). Hence, there is also a progressive increase in the surface area of the active mass. This explains the increase in the self-discharge current upon cycling (Fig. 3). These changes in the surface area of the graphite particles reach a steady state (a higher surface area than the initial state) and, thereby, the self-discharge current stabilizes at relatively high values, as seen in Fig. 3.

It should be emphasized that the behavior described above and summarized in Fig. 3 relates to 'normal' systems comprised of high purity solutions, a high ratio between the electrodes' surface area and the solution volume (i.e., a rela-

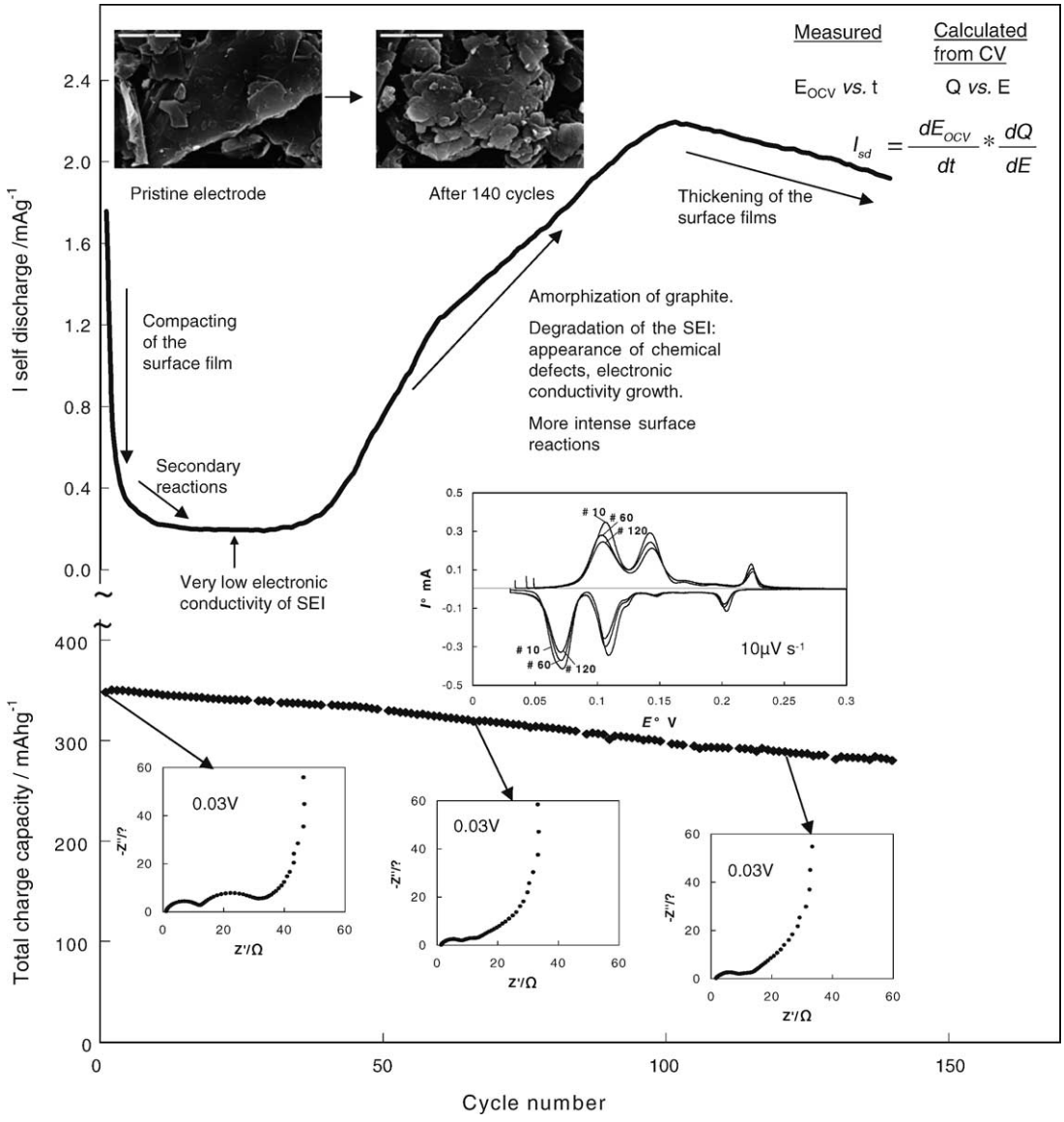

Fig. 3. A summary of experiments with a graphite electrode (composed of synthetic flakes) in an EC-DMC/$LiPF_6$ 1 M solution at RT The self-discharge current measured at each cycle from the fully lithiated electrode and the capacity are plotted as a function of cycle number. SSCV curves and impedance spectra (Nyquist plots) for three selected cycles and SEM micrographs of the pristine and the cycled electrode are also presented in the figure.

tively low impact of impurities) and well prepared electrodes (thin, compact, with good electrical inter-particle contact). There are complications related to thick and non-uniform electrodes and solutions containing impurities (H_2O, HF and other acidic or protic species). As already described, such systems may develop high impedance during cycling and capacity-fading, which results from the isolation of graphite particles by passivating surface films [34]. A high level of impurities means pronounced secondary reactions that may change the properties of the surface films, e.g., to semi conductors, which means high rates of self-discharge and the build up of thick surface films. In addition, the effect of temperature on the passivating properties of the surface films is very pronounced. At elevated temperatures, surface species dissolve, the surface chemistry may change and the electrical conductivity of the surface species is higher (i.e., higher self-discharge rates and, thus, more pronounced capacity-fading).

3.3. The preparation of nanomaterials for Li-ion batteries

The use of nanomaterials in composite electrodes for Li batteries means, on one hand, very short diffusion length and low charge transfer resistance due to the high surface area of the active mass. On the other hand, since most electrode materials for Li/Li-ion batteries are expected to be reactive with all standard solutions (comprising polar aprotic solvents and conventional Li salts), the high surface area of nanoparticles also means pronounced surface reactions and, thus, a

high level of irreversibility. Another critical point is the ease of production and cost effects.

In order to be practical, materials for batteries have to be sufficiently cheap and their synthesis has to be as simple as possible. Below, we describe some efforts made to develop nanomaterials for Li batteries.

3.3.1. Tin–carbon composites

Mesoporous carbon (MSPC) particles were prepared using SBA-15 (which is a known type of porous silicon [35]) as a template. Its synthesis was carried out according to the work of Zhao et al. [35]. Samples of as-prepared SBA-15 were calcined at 500 °C for 6 h and were mixed with an aqueous solution containing sulfuric acid and sucrose. After sonication in an ultrasonic bath, the suspension was heated at 100 °C for 6 h and later at 200 °C for 6 h. The annealed black solid material was annealed at 900 °C (Ar), thus forming a carbon–silica composite. The silica was removed by NaOH solution in a mixture of water and ethanol, leaving out the mesoporous carbon. For the insertion of SnO into the MSPC particles, the latter were mixed with a solution of tin chloride and $SnCl_2$, in ethanol. The solution was sonicated in an ultrasonic bath for 30 min, after which the ethanol was evaporated and the residue was heated at 530 °C under argon for 2 h. The product underwent the regular characterization process, including wide angle XRD, TEM and BET measurements.

Fig. 4 summarizes several important experimental results related to this material. The XRD patterns show a typical Sn peak, meaning that we obtained a reduction of SnO, probably by ethanol. The TEM image shows the unique morphology of these particles. The pristine carbon material is inactive in Li insertion, while the C–Sn composite shows very stable and reversible lithiation in which the Sn particles, embedded in the carbon matrix, play a key role. An overall reversible capacity around 400 mAh g^{-1} could be obtained, meaning that the lithiation of the tin is close to the theoretical capacity of $Li_{4,4}Sn$ (the Sn/C ratio was around 1/3) [36].

3.3.2. SnS

Nanoparticles of SnS could be synthesized by reacting H_2NCSNH_2 with $SnCl_2$ in an aqueous medium using microwave radiation. The following is the mechanism:

$$H_2NCSNH_2 + 2H_2O \rightarrow CO_2 + 2NH_3 + H_2S$$

and

$$SnCl_2 + H_2S \rightarrow SnS + 2HCl.$$

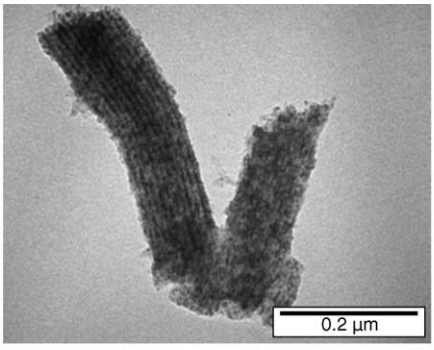

(A) TEM images of a Tin-Mesoporous carbon particle

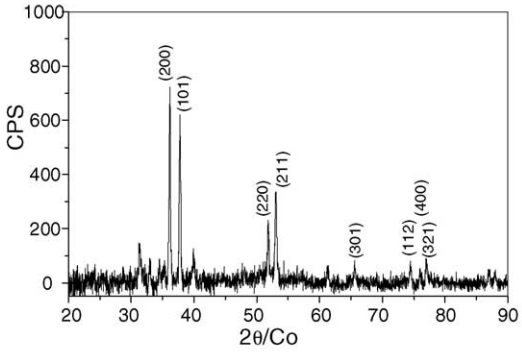

(B) XRD pattern of the Sn/MSPC matrix

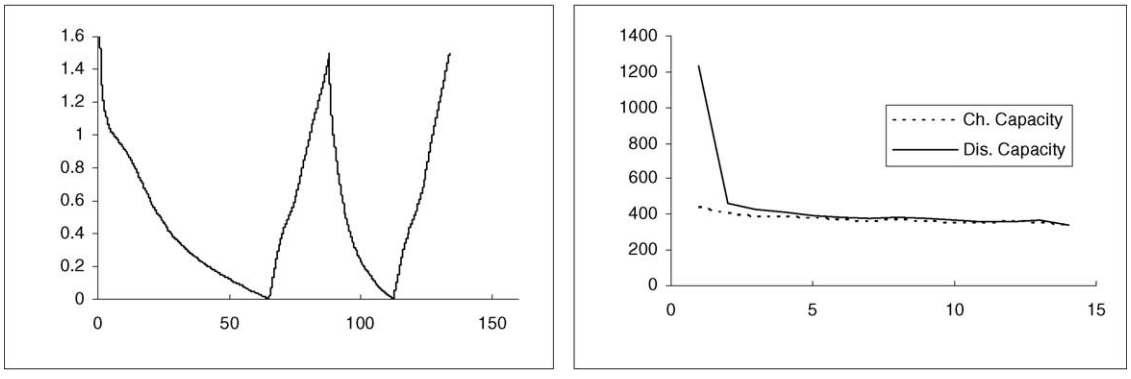

(C) Galvanostatic measurements of Tin-mesoporous carbon (C/20) electrodes

Fig. 4. Several key data related to the Sn–mesoporous carbon (MSPC) anode material: (A) TEM image of a single particle, (B) XRD pattern of the active mass, which in fact relates to metallic tin particles and (C) galvanostatic cycling in an EC-DMC/$LiPF_6$ 1 M solution of a composite electrode comprising the active mass and PVdF binder (9:1). *C*/10 rate, 25 °C, the voltage profile and the capacity vs. cycle number are presented.

SnS particles of high purity could be obtained as nanoflakes. Composite electrodes comprising SnS, carbon and a PVdF binder (8:1:1, w/w/w), could be cycled in alkyl carbonates/Li salt solutions and demonstrated reversible lithiation–delithiation stable cycling, with a capacity around 600 mAh g^{-1}.

3.3.3. VO_x compounds

We developed a series of reactions under autogenic pressure at elevated temperatures that could be carried out in very simple reactors. $VO(OC_2H_5)_3$ was heated to 700 °C during 1 h in a closed metallic vessel and produced carbon coated V_2O_3 nanoparticles.

The carbon coating around these nanoparticles (50 nm average particle size) was 10–15 nm thick and was permeable to Li-ions because the carbon interlayer spacing was sufficiently large, >3.8 Å. Thus, this material was found to be electrochemically active and intercalates reversibly with lithium at potentials between 2 and 4 V. The oxidation of this material in air produced γ-V_2O_5 coated with a thin carbon layer (a few nm thick and active in non-aqueous Li salt solutions):

$$\text{carbon coated } V_2O_3 \xrightarrow{400^\circ C,\ \text{air}} CCV_2O_5$$

Cycling CCV_2O_5 as the active mass in composite electrodes in non-aqueous Li salt solutions (e.g., PC/$LiClO_4$) between 2 and 4 V (Li/Li^+) produced an irreversible phase transition to ω-$Li_xV_2O_5$ that could be lithiated and delithiated repeatedly at very stable capacities close to 300 mAh g^{-1}. The production procedure of the CCV_2O_5 can be easily upscaled to obtain large quantities.

Electrochemically active nano VO_x materials could also be produced by sonochemistry. $(iPrO)_3VO$ under sonic radiation in a de-aerated water medium decomposes to V_3O_7 nanoparticles, which are electroactive in Li salt solutions [37]. Heating this material in air (300 °C) produced highly pure nanoparticles of γ-V_2O_5 that intercalate with lithium reversibly, as expected.

4. Conclusions

Standard $LiPF_6$ solutions (in mixtures of alkyl carbonates such as EC-EMC, EC-DMC and EC-DEC-DMC) can be used at elevated temperatures in Li-ion batteries, by adding to them organosilicon compounds that react with trace HF and water in the bulk and, hence, avoid the detrimental impact of acidic contaminants on the electrodes' performance in Li-ion batteries. It should be emphasized that the weak side in Li-ion batteries, upon cycling at high temperatures (e.g., 60 °C), is the Li–carbon anode (failure through isolation of graphite particles by electronically insulating surface films). Thus, the most important impact of these additives is improving the cycleability of the Li–C anodes. However, there is also a positive impact on $LiCoO_2$ electrodes (reduction of Co ion dissolution during prolonged cycling and prevention of high impedance). Standard $LiPF_6$ solutions can also be used for 5 V cathodes such as $LiMn_{1.5}Ni_{0.5}O_2$, where a cut-off voltage below 4.85 V (Li/Li^+) is sufficient to extract all the capacity.

We described herein changes in the safe discharge current, measured from lithiated graphite electrodes during prolonged cycling, which reflect two opposing processes. The surface films and the electrodes' passivation should naturally stabilize during cycling if the morphology of the active mass is stable. However, prolonged cycling, even in the best systems, leads to cracking, disordering and some amorphization of the graphite active mass near the surface and, hence, increases the active surface area of the graphite particles. Thereby, the self-discharge current initially drops during cycling, stabilizes at low values and then rises and stabilizes at high values due to the increase in the electrodes' surface area.

Finally, we examined several types of nanomaterials for Li-ion batteries, including mesoporous carbon particles filled with tin, SnS nanoparticles and V_2O_5 nanoparticles. The common denominator in these efforts was the promising performance of composite electrodes comprising these materials in reversible and stable repeated lithiation–delithiation cycling and synthetic routes that are relatively cheap, simple and can be upscaled to large quantities.

Acknowledgment

This work was supported by Merck KGaA (collaboration with Dr. W. Geissler is acknowledged), LG-Korea (collaboration with Dr. H.J. Kim is acknowledged) and the European Commission, in various projects within the framework of the fifth Program.

References

[1] J. Graetz, C.C. Ahn, R. Yazami, B. Fultz, Electrochem. Solid-State Lett. 6 (2003) A194.
[2] J.H. Kim, G.J. Jeong, Y.W. Kim, H.J. Sohn, C.W. Park, C.K. Lee, J. Electrochem. Soc. 150 (2003) A1544.
[3] L.F. Nazar, O. Crosnier, in: G.A. Nazri, G. Pistoia (Eds.), Lithium Batteries, Science and Technology, Kluwer Academic Publishers, Boston, NY, London, 2004, p. 129 (Chapter 4).
[4] J. Yin, M. Wada, S. Tanase, T. Sakai, J. Electrochem. Soc. 151 (2004) A867.
[5] N. Li, D.T. Mitchell, K.P. Lee, C.R. Martin, J. Electrochem. Soc. 150 (2003) A979.
[6] A.S. Zhang, K. Xu, T.R. Jow, J. Power Sources 113 (2003) 166.
[7] K. Xu, S. Zhang, T.R. Jow, W. Xu, C.A. Angell, Electrochem. Solid-State Lett. 5 (2002) A26.
[8] M. Adachi, K. Tanaka, K. Sekai, J. Electrochem. Soc. 146 (1999) 1256.
[9] H. Bohm, in: J.O.B. Besenhard (Ed.), Handbook of Battery Materials, part III, Wiley/VCH, Weinheim, NY, Singapore, 1999, p. 565 (Chapter 11).
[10] B. Scrosati, in: W.A. Van Schalkwijk, B. Scrosati (Eds.), Advances in Lithium-Ion Batteries, Kluwer Academic/Plenum Publishers, NY, Boston, London, 2002, p. 251 (Chapter 8).
[11] P. Birke, W. Weppner, in: J.O.B. Besenhard (Ed.), Handbook of Battery Materials, Part III, Wiley/VCH, Weinheim, NY, Singapore, 1999, p. 525 (Chapter 9).

[12] M. Pasquadi, S. Passerini, G. Pistoia, in: G.A. Nazri, G. Pistoia (Eds.), Lithium Batteries, Science and Technology, Kluwer Academic Publishers, Boston, NY, London, 2004, p. 347 (Chapter 11).
[13] Z. Wang, Y. Sun, L. Chen, X. Huang, J. Electrochem. Soc. 151 (2004) A914.
[14] Y. Shin, A. Manthiran, Electrochim. Acta 48 (2003) 3538.
[15] M. Menetrier, C. Vaysse, C. Delmass, L. Croquennec, C. Jordy, F. Bonhomme, P. Biensan, Electrochem. Solid-State Lett. 7 (2004) A140.
[16] J.M. Kim, H.T. Chung, Electrochim. Acta 49 (2004) 3573.
[17] J.M. Jim, H.F. Chung, Electrochim. Acta 49 (2004) 937.
[18] S. Okada, S. Sawa, Y. Uebou, M. Egashira, J. Yamaki, M. Tabushi, H. Kobayashi, K. Fukumi, H. Kageyama, Electrochemistry 71 (2003) 1136.
[19] K. Dokko, Q.F. Shi, I.C. Stefan, D.A. Scherson, J. Phys. Chem. B 107 (2003) 12549.
[20] H.J. Santner, C. Korepp, M. Winter, J.O.B. Besenhard, K.C. Moller, Anal. Bioanal. Chem. 379 (2004) 266.
[21] D. Aurbach, M. Koltypin, H. Teller, Langmuir 18 (2002) 9000.
[22] T.D. Hatchard, J.R. Dahn, J. Electrochem. Soc. 151 (2004) A838.
[23] M. Lanz, P. Novak, J. Power Sources 102 (2001) 277.
[24] W.S. Yoon, S. Iannopollo, C.P. Grey, D. Carlier, J. Gorman, J. Reed, G. Ceder, Electrochem. Solid-State Lett. 7 (2003) A167.
[25] J.M. Vollmer, L.A. Curtiss, D.R. Vissers, K. Amine, J. Electrochem. Soc. 151 (2004) A178.
[26] D. Aurbach, B. Markovsky, M.D. Levi, E. Levi, A. Schechter, M. Moshkovich, Y. Cohen, J. Power Sources 81–82 (1999) 95.
[27] D. Aurbach, Y. Gofer, Y. Langzam, J. Electrochem. Soc. 136 (1989) 3198.
[28] D. Aurbach, B. Markovsky, K. Gamolsky, E. Levi, Y. Ein-Eli, Electrochim. Acta 45 (1999) 67.
[29] D. Aurbach, K. Gamolsky, B. Markovsky, G. Salitra, Y. Gofer, J. Electrochem. Soc. 147 (2000) 1322.
[30] S.H. Ma, H. Noguchi, M. Yoshio, J. Power Sources 125 (2004) 228.
[31] J.S. Gnanaraj, E. Zinigrad, L. Asraf, H.E. Gottlieb, M. Sprecher, M. Schmidt, W. Geissler, D. Aurbach, J. Electrochem. Soc. 150 (2003) A1533.
[32] J.W. Jiang, H. Fortier, J.N. Reimers, J.R. Dahn, J. Electrochem. Soc. 151 (2004) A609.
[33] D. Aurbach, B. Markovsky, A. Rodkin, G. Salitra, Y. Tal-Yosef, H.J. Kim, J. Electrochem. Soc. 151 (2004) A1068.
[34] D. Aurbach, B. Markovsky, A. Rodkin, M. Cojocaru, E. Levi, H.J. Kim, Electrochim. Acta 47 (2002) 1899.
[35] D. Zhao, J. Sun, Q. Li, G.D. Stucky, Chem. Mater. 12 (2000) 275.
[36] I. Grigoriants, L. Sominski, H. Li, I. Ifargan, D. Aurbach, A. Gedanken, Chem. Comm. 7 (2005) 921.
[37] D. Aurbach, A. Nimberger, B. Markovsky, A. Odani, E. Sominski, E. Levi, V.G. Kumas, M. Motiei, A. Gedanken, P. Dan, J. Power Sources 119–121 (2003) 517.